[Electronic Supplementary Information]

Anomalous proton transfer of a photoacid HPTS in nonaqueous reverse micelles

Taehyung Jang, Sebok Lee, and Yoonsoo Pang*

Department of Chemistry, Gwangju Institute of Science and Technology, 123 Cheomdangwagi-ro, Buk-gu, Gwangju 61005, Republic of Korea

Table of Contents

1. Dynamic light scattering measurements of *water-in-oil* and *methanol-in-oil* RMs

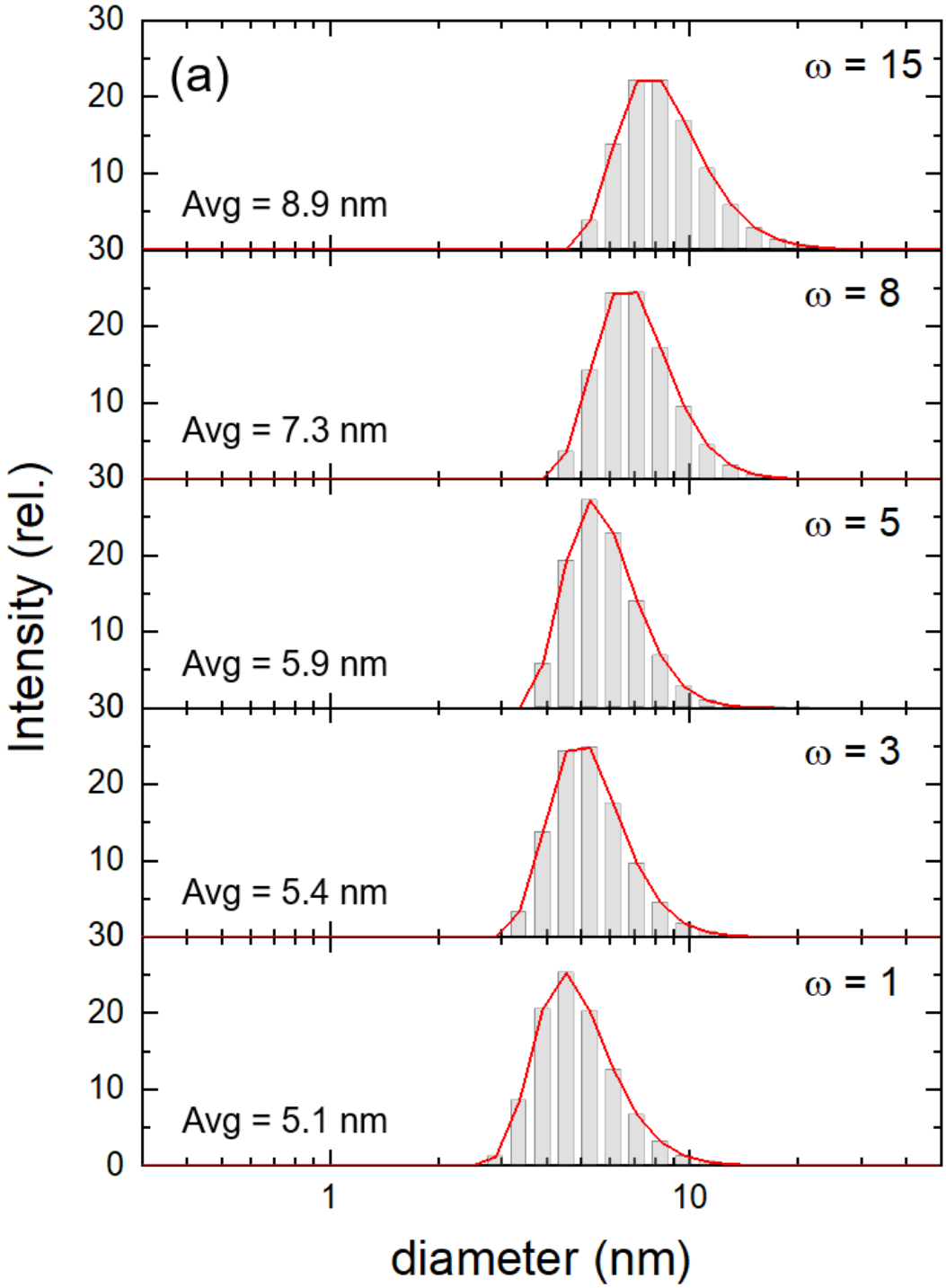

Fig. S1 Distribution of the micelle diameter of the *water-in-oil* RMs with the surfactant Igepal CO-520 obtained from the dynamic light scattering (DLS) measurements.

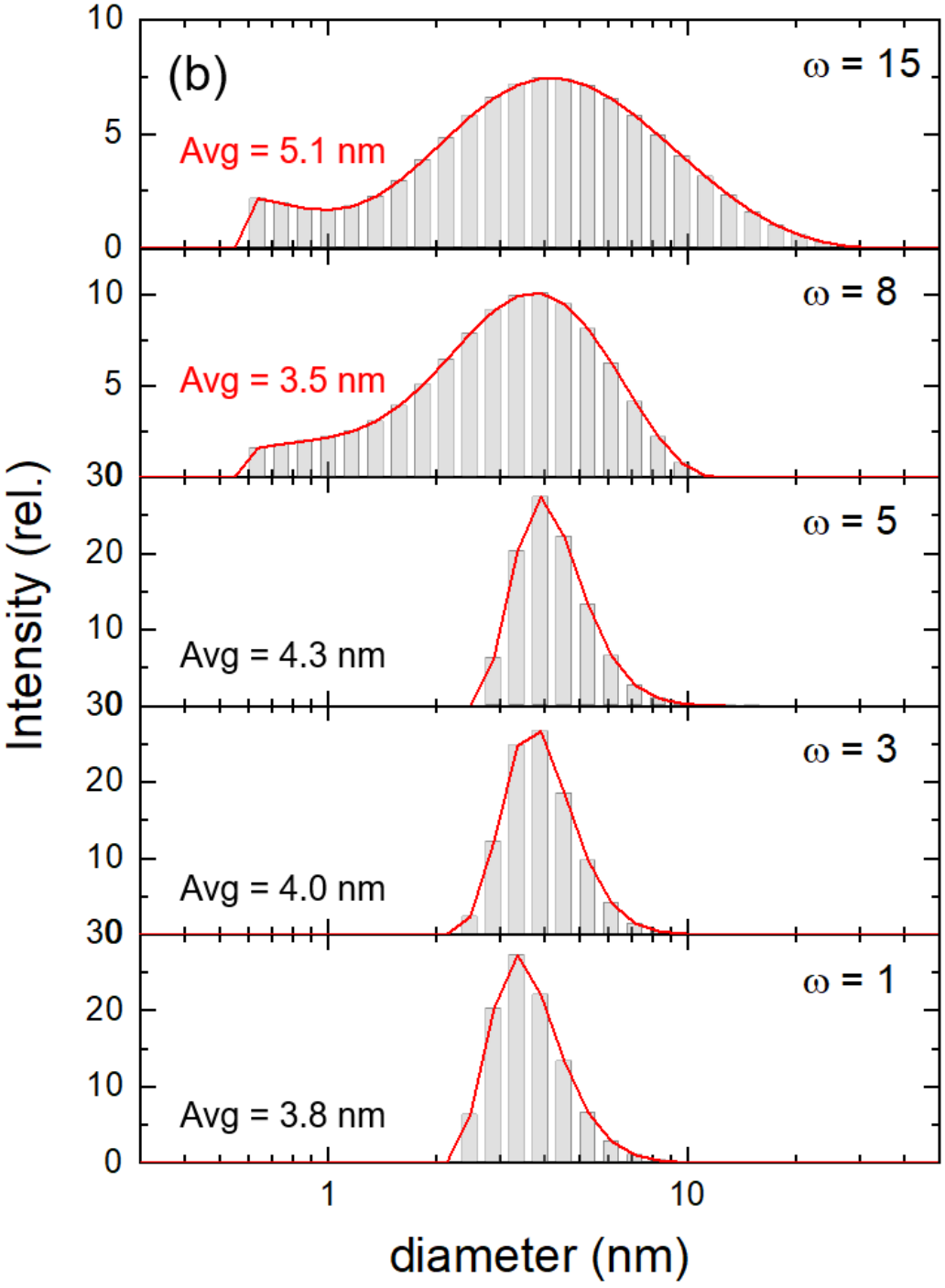

Fig. S2 Distribution of the micelle diameter of the *methanol-in-oil* RMs with the surfactant Igepal CO-520 obtained from the dynamic light scattering (DLS) measurements.

2. Absorption and emission spectra of HPTS in *water-in-oil* AOT RMs and methanol solution of Igepal CO-520

Fig. S3 represents the steady-state absorption and emission spectra of HPTS obtained in *water-in-oil* RMs composed of the surfactant AOT.

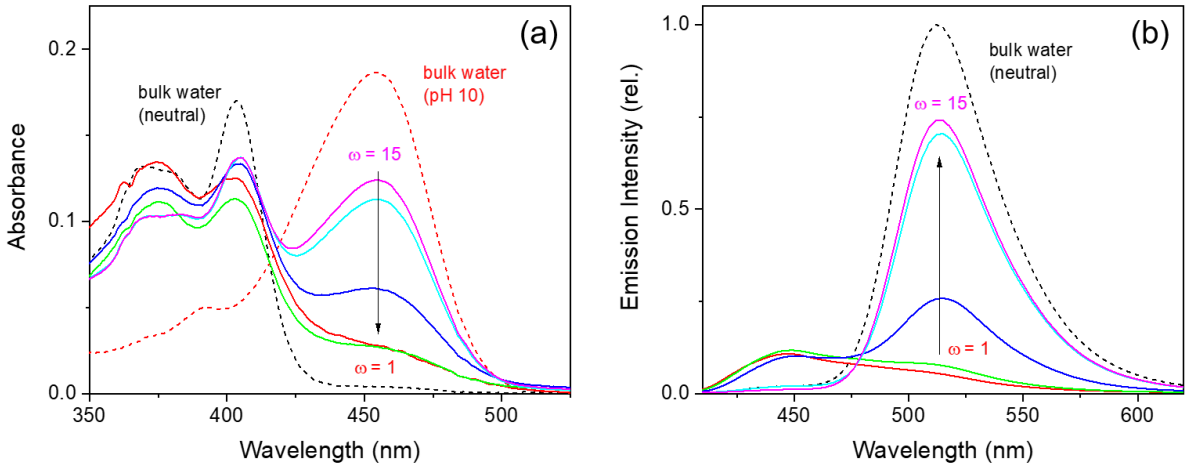

Fig. S3 (a) Steady-state absorption and (b) emission spectra of HPTS (1×10^{-5} M) in water/AOT/isooctane reverse micelles (RMs) of ω = 1, 3, 5, 8, and 15 (solid lines). The excitation at 405 nm was used for the emission measurements and all the emission spectra were normalized with respect to the absorbance value of each sample at 405 nm. The absorption and emission spectra of HPTS in the bulk aqueous solutions (dashed lines) of neutral and basic pHs were also compared.

Fig. S4 shows the steady-state absorption and emission spectra of HPTS in ω = 1 *methanol-in-oil* RMs, bulk methanol, Igepal/methanol mixture, and Igepal only. The final concentration of HPTS was kept as 10 μM for all samples (except HPTS in Igepal only due to the low solubility). The absorption spectra of HPTS in bulk methanol, methanol/Igepal mixture are very similar to that of the ω = 1 *methanol-in-oil* RMs without the deprotonated band. The absorption spectrum of HPTS in Igepal only does not show the deprotonated band either, but the absorption maximum at 402 nm appears slight blue-shifted from the other spectra. The emission spectrum of HPTS in the ω = 1 *methanol-in-oil* RMs shows a substantial deprotonated emission band at 507 nm while the spectra in bulk methanol and Igepal/methanol mixture show no deprotonated band. The emission spectrum in Igepal only is similar to the neutral emission spectra obtained in bulk methanol and Igepal/methanol mixture, and the quantum yield of HPTS decreases largely due to strong fluorescence quenching. The disappearance of deprotonated emission band, a much smaller quantum yield, and slight blue-shift in the absorption band all represent that HPTS in small *methanol-in-oil* RMs mainly exist inside the micelle core and that the portion of probe molecules trapped between the Igepal surfactants is considered negligible. Since the tail group of the surfactant Igepal CO-520 would be considered a fairly weak base (with ether and primary alcohol groups),[1] the direct interaction between HPTS and the tail groups of Igepal CO-520 surfactant would be considered unfavorable compared to the solvation inside the *methanol-in-oil* RMs.

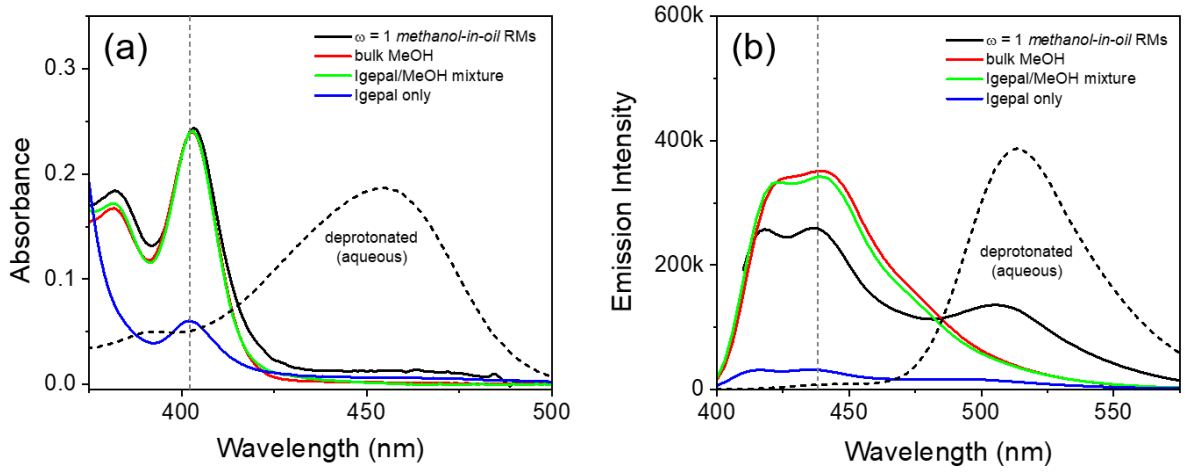

Fig. S4 Steady-state (a) absorption and (b) emission spectra of HPTS in ω = 1 *methanol-in-oil* RMs, bulk methanol, Igepal/methanol mixture, and Igepal only. The absorption and emission spectra of the deprotonated HPTS in aqueous solution (dashed lines) are shown for comparison. The excitation at 405 nm was used for the emission measurements.

3. Ground- and excited-state pK_a of HPTS in aqueous and methanol solutions

Determination of the ground- and excited-state pK_a values of acids and bases in various solvents have often been investigated by the spectrophotometric methods.[2-4] The reversible changes in the absorption and emission intensities of the protonated or deprotonated species depending on the solution pH are recorded, and the pK_a values can be estimated as the pH values at the inflection points in the absorption or emission intensity of the deprotonated or protonated species. The dissociation of a proton from an acid (HA) can be related to the solution pH by the following equation known as Henderson-Hasselbach equation.

$$\mathrm{pH} = \mathrm{p}K_a + \log\frac{[\mathrm{A}^-]}{[\mathrm{HA}]} \quad (1)$$

With the fraction for the deprotonated species A^-, $f_{\mathrm{A}^-} = \left[\mathrm{A}^-\right] \Big/ \left(\left[\mathrm{HA}\right] + \left[\mathrm{A}^-\right]\right)$, equation 1 can be modified as Hill equation,

$$f_{\mathrm{A}^- \text{ or HA}} = \frac{1}{1+10^{n(\mathrm{pH}-\mathrm{p}K_a)}} \quad (2)$$

where the Hill coefficient n is -1 for the deprotonated species A^- and +1 for the protonated species HA. The Hill coefficient has been used as a stretch parameter to fit non-ideal titration data for the protonated and deprotonated species of acids and bases.[3, 5]

The absorption and emission spectra of HPTS in the aqueous or methanol solutions of 5.0×10^{-5} M in a wide range of the solution pH were obtained by using the stock solutions of 1-10 M HCl or NaOH prepared with water or methanol. Fig. S5 shows the pK_a evaluation of HPTS in the aqueous solution by the absorption and emission spectra. The ground state pK_a value of HPTS in the aqueous solution was determined from the fractions of protonated and deprotonated absorption bands centered at 403 and 454 nm, respectively, as shown in Fig. S5(a). From the titration curve shown in Fig. S5(c), the ground state pK_a value of HPTS in the aqueous solution was evaluated as 7.9, which is quite similar to the previously reported value of 7.7.[6, 7]

The excited-state pK_a^* value of HPTS in the aqueous solution was determined from the emission intensities of protonated and deprotonated bands at 450 and 512 nm, respectively, as shown in Fig. S5(b). The pK_a^* of HPTS in the aqueous solution was evaluated as 0.8 as shown in Fig. S5(d), which is quite similar to the previously reported value of 0.5.[6, 7]

Figs. S6(a) and S6(b) show the absorption and emission spectra of HPTS in the methanol solution. The ground state pK_a value of HPTS in the methanol solution was determined as 11.4 from the absorbance fractions of the protonated and deprotonated absorption bands centered at 403 and 454 nm, respectively, as shown in Fig. S6(c). Similarly, the excited-state pK_a^* value of HPTS in the methanol solution was determined as 11.8 from the intensity fractions of the protonated (440 nm) and deprotonated emission bands (512 nm), as shown in Fig. S6(d). However, more precise estimation for the excited-state pK_a^* values would be made by measuring the rate constant for the proton transfer by time-resolved spectroscopic methods.[8, 9] Since the excited-state proton transfer (ESPT) of HPTS in methanol is too small to be measured by any electronic spectroscopy, the estimation of the proton transfer rate constant $k_{PT} \sim 5\times10^6$ s^{-1} has been made by the spectral measurements of the water-methanol binary mixtures.[9] The pK_a^* values of ~4 has been estimated from the proton transfer rate constant (k_{PT}) in methanol by the Marcus relation for nonadiabatic electron transfer and the free energy correlation scheme.[9]

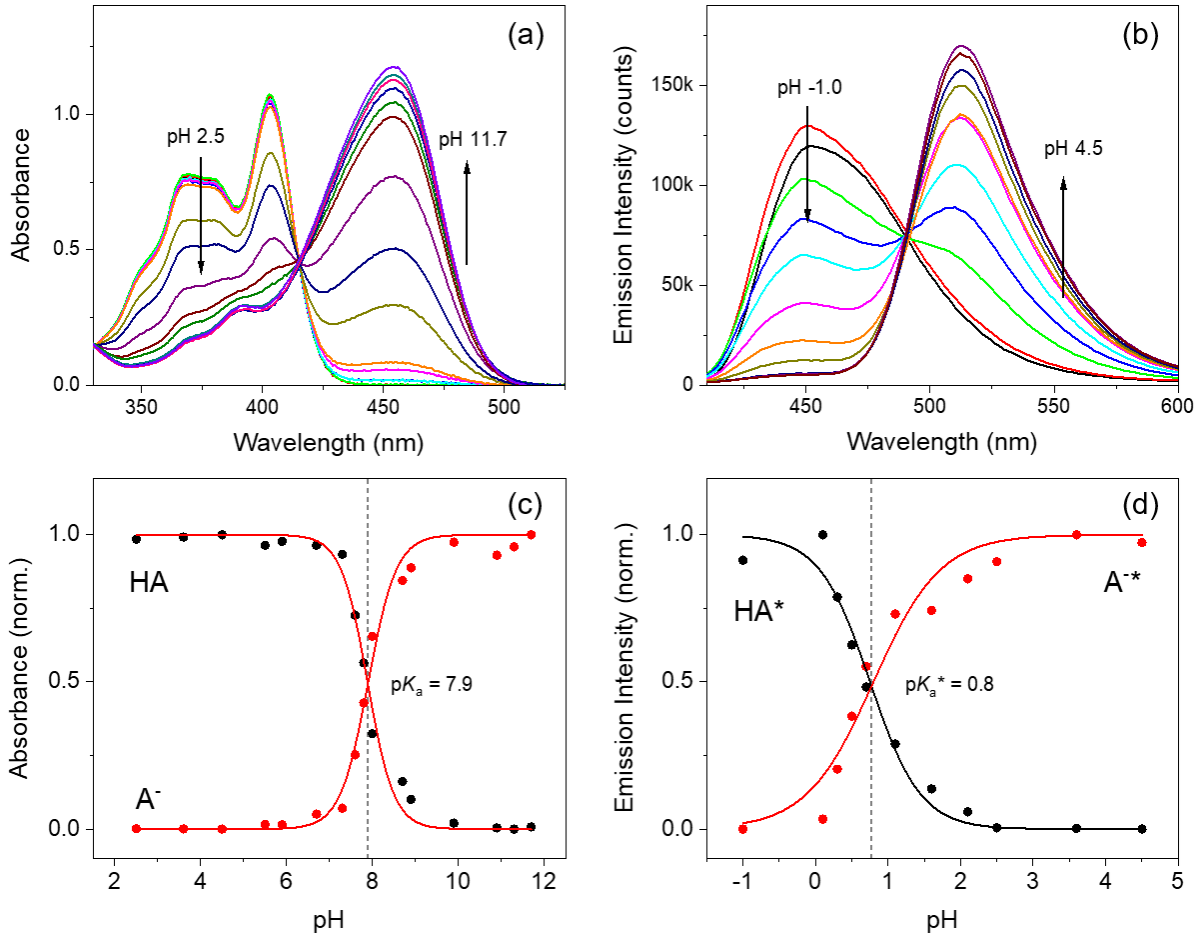

Fig. S5 The pK_a values of HPTS in the aqueous solution in the ground and excited state; (a) steady-state absorption and (b) emission spectra of HPTS obtained in the wide range of the solution pHs, (c) the ground state pK_a determined from the inflection points in the absorbance fractions of the protonated (403 nm) and deprotonated bands (454 nm), (d) the excited-state pK_a^* determined from the inflection points in the intensity fractions of the protonated (450 nm) and deprotonated emission bands (512 nm). The excitation at 405 nm was used for the emission measurements.

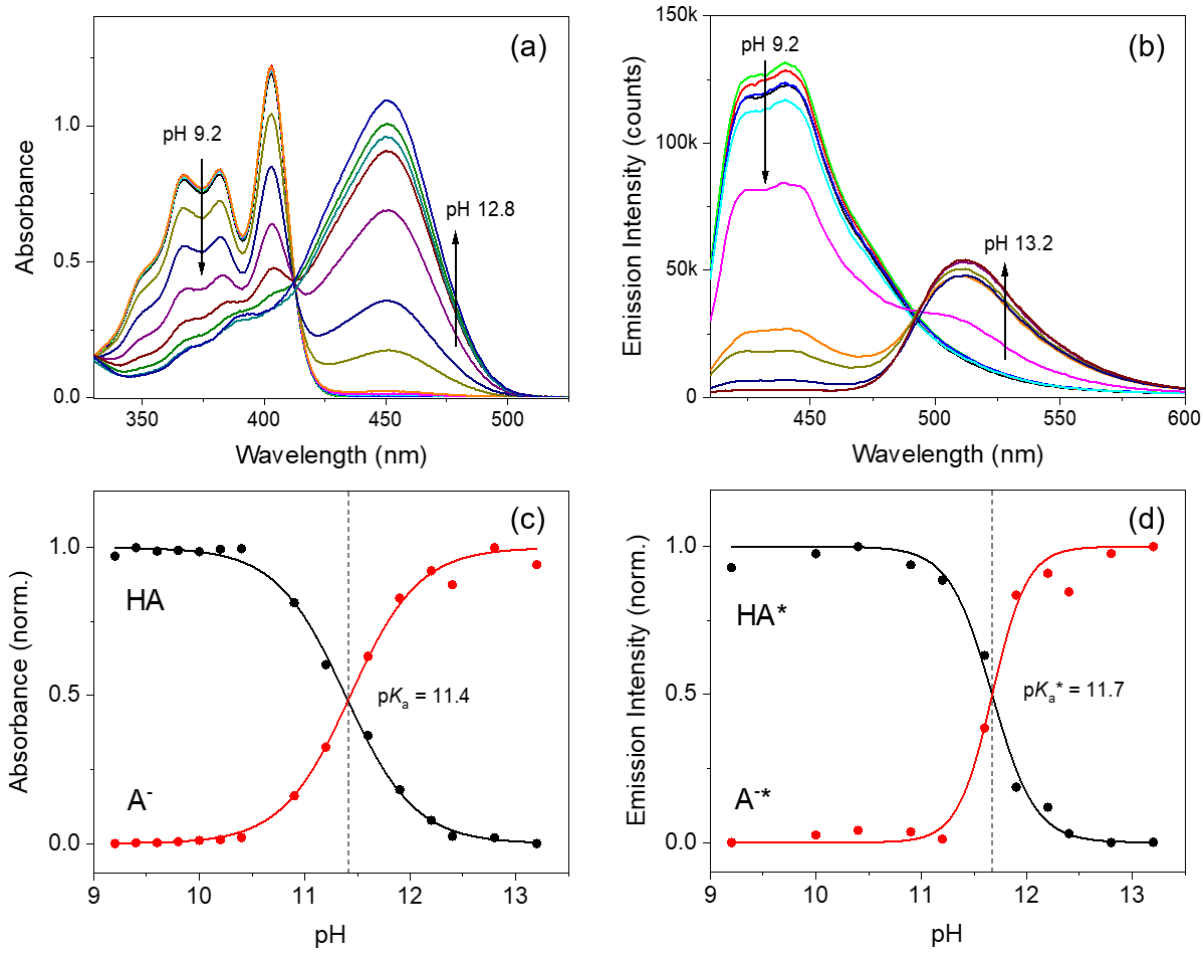

Fig. S6 The pK_a values of HPTS in the methanol solution in the ground and excited state; (a) steady-state absorption and (b) emission spectra of HPTS obtained in the wide range of the solution pHs, (c) the ground state pK_a determined from the inflection points in the absorbance fractions of the protonated (403 nm) and deprotonated bands (454 nm), (d) the excited-state pK_a^* determined from the inflection points in the intensity fractions of the protonated (440 nm) and deprotonated emission bands (512 nm). The excitation at 405 nm was used for the emission measurements.

4. Fluorescence anisotropy of HPTS in *methanol-in-oil* RMs

The fluorescence anisotropy results for the protonated species of HPTS in *methanol-in-oil* RMs and bulk methanol probed at 440 nm with the 405 nm excitation were shown in Fig. S7. The fluorescence anisotropy in bulk methanol shows a single-exponential decay of 0.20 ns. The anisotropy results in the *methanol-in-oil* RMs were fit with the bi-exponential decays, where the rotational dynamics of dye molecules in the RMs can be interpreted as the wobbling-in-a-cone model.[6, 10-12] Table S1 summarizes the fluorescence anisotropy of HPTS in *methanol-in-oil* RMs and bulk methanol. The protonated species of HPTS in *methanol-in-oil* RMs show bi-exponential decays of 0.85 and 2.08 ns for $\omega = 5$ RMs and 1.48 and 4.40 ns for $\omega = 1$ RMs. The wobbling time (τ_w) and semi-cone angle (θ) of HPTS in *methanol-in-oil* RMs show size dependence (1.45 ns, 47.6° for $\omega = 5$; 2.2 ns, 45.4° for $\omega = 1$), which are similar to the previous results of *water-in-oil* Igepal RMs.[6] Considering the previous time-resolved fluorescence anisotropy results of HPTS in anionic and nonionic RMs, and cationic (BHDC) RMs, the electrostatic interactions between surfactant head groups and (neutral or anionic) HPTS molecules strongly affects the probe dynamics inside the nanopools.[6, 13] In anionic AOT RMs, HPTS molecules would exist in the core of RMs with freely rotating motions (large semi-cone angles, θ = 59-60°) due to strong electrostatic repulsions. On the other hand, the strong electrostatic interactions between cationic head groups of BHDC and HPTS strongly restrict the wobbling motion of probe molecules (much smaller semi-cone angles, θ = 13-23° compared to the anionic RMs). In nonionic Igepal RMs, the semi-cone angle for the wobbling motion (θ = 42-45°) appears smaller than those of anionic RMs (but much larger than those of cationic RMs). Thus, HPTS molecules are considered to exist inside the Igepal RMs with slight interactions with the head groups of Igepal.

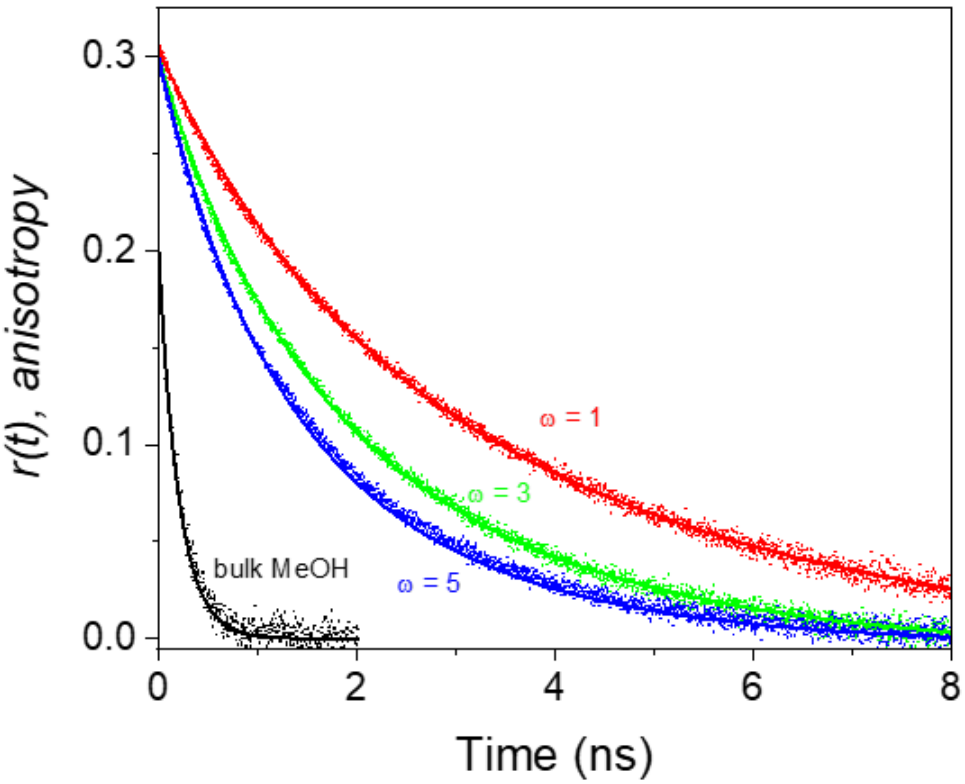

Fig. S7 Fluorescence anisotropy for the protonated species of HPTS in the *methanol-in-oil* RMs (ω = 1, 3, and 5) and bulk methanol were probed at 440 nm with the 405 nm excitation.

Table S1. Fluorescence anisotropy decay parameters of HPTS in *methanol-in-oil* RMs and bulk methanol

	r_0	S^2	τ_{slow} (ns)	τ_{fast} (ns)	τ_w (ns)	θ (deg)
RMs (ω = 1)	0.31	0.71	4.40 ± 0.05	1.48 ± 0.05	2.2 ± 0.1	45.4
RMs (ω = 3)	0.30	0.65	2.79 ± 0.04	1.07 ± 0.03	1.74 ± 0.06	47.1
RMs (ω = 5)	0.30	0.63	2.08 ± 0.03	0.85 ± 0.03	1.45 ± 0.07	47.6
bulk methanol	0.21	-	-	0.20 ± 0.00	-	-

5. Excited-state proton transfer (ESPT) dynamics of HPTS in the RMs

The ESPT dynamics of HPTS were analyzed based on the two-step proton transfer model, which has been extensively used in previous studies.[6, 14-17] The two-step proton transfer model shown below includes the formation of the contact ion pair $[H^+\cdots A^-]$ and the dissociation of the proton in the excited state. The time-dependent changes in the concentration of excited-state species of HPTS, HA^*, $[H^+\cdots A^-]^*$, and A^{-*}, are described in the following set of differential equations with the rate constants of k_{PT}, k_{rec}, k_{diss}, k_{pr}, k_{HA}, and k_{A^-},

$$\frac{d}{dt}\begin{pmatrix}[HA]^* \\ [H^+\cdots A^-]^* \\ [A^-]^*\end{pmatrix} = \begin{pmatrix}-X & k_{rec} & 0 \\ k_{PT} & -Y & k_{pr}[H^+]_w \\ 0 & k_{diss} & -Z\end{pmatrix}\begin{pmatrix}[HA]^* \\ [H^+\cdots A^-]^* \\ [A^-]^*\end{pmatrix} \quad (3)$$

where X, Y, and Z represent the sums of the following rate constants.

$$X = k_{PT} + k_{HA} \quad (4)$$

$$Y = k_{rec} + k_{diss} + k_{A^-} \quad (5)$$

$$Z = k_{pr}[H^+]_w + k_{A^-} \approx k_{A^-} \quad (6)$$

Since the protonation rate of A^{-*} also depends on the concentration of the proton $[H^+]_w$, the protonation rate term $k_{pr}[H^+]_w$ can be neglected in most cases except the acidic conditions (pH < 3).[18]

The solution of the differential equations for the excited-state species of HPTS can be obtained by finding out the eigenvalues and eigenvectors for the 3×3 rate constant matrix shown in eqn. 3. Three eigenvalues λ_1-λ_3 can be obtained by solving the following determinant equation.

$$\begin{vmatrix}\lambda - X & k_{rec} & 0 \\ k_{PT} & \lambda - Y & 0 \\ 0 & k_{diss} & \lambda - Z\end{vmatrix} = 0 \quad (7)$$

$$\lambda_{2,1} = \frac{(X+Y) \pm \sqrt{(X-Y)^2 + 4k_{rec}k_{PT}}}{2} \tag{8}$$

$$\lambda_3 = Z = k_{A^-} \tag{9}$$

The time constants and amplitudes for the multi-exponential fluorescence decay of HA^* can be interpreted as the proton transfer and recombination rate constants used in the differential equation by evaluating the eigenvectors of each eigenvalue of the rate constant matrix.

$$[HA]^* = A_1 e^{-\lambda_1 t} + A_2 e^{-\lambda_2 t} \tag{10}$$

The derivation of all the rate constants are summarized as the following equations, where the amplitude ratio between the first and second time constants for HA^*, $R = A_2/A_1$ was introduced.

$$X = \frac{\lambda_1 + R\lambda_2}{1+R} \tag{11}$$

$$Y = \lambda_1 + \lambda_2 - X = \frac{\lambda_2 + R\lambda_1}{1+R} \tag{12}$$

The proton transfer and recombination rate constants of HPTS in the excited state can be written as the experimental fit results (amplitudes and time constants) for the protonated species of HPTS from time-resolved fluorescence and transient absorption measurements,

$$k_{PT} = X - k_{HA} \approx X = \frac{1/\tau_1 + R/\tau_2}{1+R} \tag{13}$$

$$k_{rec} = \frac{XY - \lambda_1\lambda_2}{X} = \frac{1/\tau_2 + R/\tau_1}{1+R} - \frac{1}{X\tau_1\tau_2} \tag{14}$$

$$k_{diss} = Y - k_{A^-} - k_{rec} = \frac{1}{X\tau_1\tau_2} - \frac{1}{\tau_6} \tag{15}$$

where the time constant τ_6 denotes the excited-state decay time constant of the deprotonated species of HPTS (A^{-*}).

6. Solvation dynamics of HPTS in *water-in-oil* and *methanol-in-oil* RMs

Transient absorption results of HPTS in *water-in-oil* and *methanol-in-oil* RMs in Fig. 5 were analyzed by the dynamic Stokes' shifts of the protonated ESA bands. The frequency correlation function, *C(t)* was calculated from the center frequency of the protonated ESA band at each time delay as,

$$C(t) = \frac{\nu(t) - \nu(\infty)}{\nu(0) - \nu(\infty)} \tag{16}$$

where ν(0) and ν(∞) represent the center frequencies of the ESA band at zero and infinite time delays, respectively. The resulting correlation functions shown in Fig. S8 were fit to single exponential functions of which time constants were interpreted as the solvation dynamics components of HPTS in bulk solvents and confined solvents in the RMs. In bulk water, a 0.46 ps component was retrieved from the dynamic Stokes' shifts, which is quite similar as the fastest (0.44 ps) component in the global analysis results shown in Fig. 6. The previously reported values from femtosecond transient absorption and fluorescence upconversion spectroscopy are 0.3 ps[17, 19, 20] and 0.98-0.99 ps.[14, 16] Similarly, the solvation dynamics of 1.5 and 3.7 ps were retrieved from the dynamic Stokes' shifts of HPTS in ω = 15 and ω = 1 *water-in-oil* RMs, respectively. The kinetic components (1.6 and 3.7 ps) from the global analysis of transient absorption results of HPTS in ω = 15 and ω = 1 *water-in-oil* RMs, respectively, appear identical to the dynamic Stokes' shift results. The solvation dynamics of 2.1 and 2.7 ps were retrieved from the dynamic Stokes' shifts of HPTS in ω = 15 and ω = 1 *methanol-in-oil* RMs, respectively.

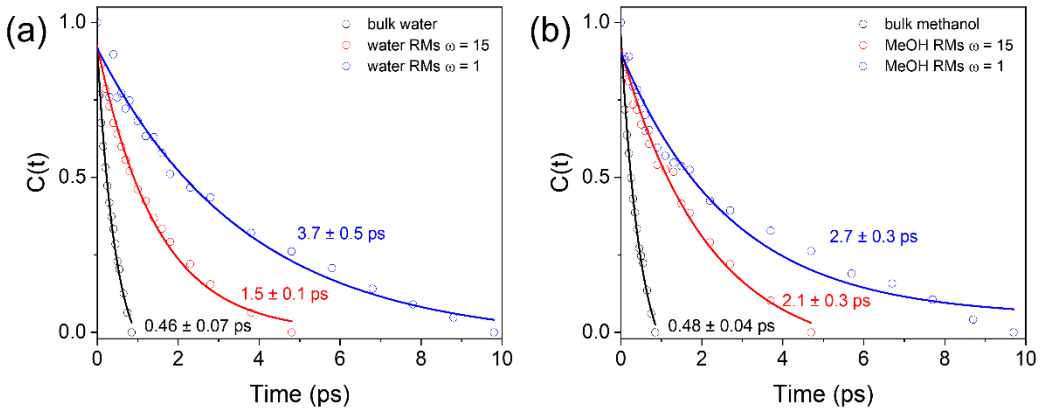

Fig. S8 The dynamic Stokes' shifts of HPTS in (a) bulk water and *water-in-oil* RMs and (b) bulk methanol and *methanol-in-oil* RMs obtained from the protonated ESA bands of transient absorption results.

References

1. P. Y. Bruice, *Essential Organic Chemistry*, Prentice Hall2010.
2. M. Hasegawa, *Langmuir*, 2001, **17**, 1426-1431.
3. C. D. Sanborn, J. V. Chacko, M. Digman and S. Ardo, *Chem*, 2019, **5**, 1648-1670.
4. L. G. T. A. Duarte, J. C. Germino, C. d. Á. Braga, C. A. Barboza, T. D. Z. Atvars, F. d. S. Santos and F. S. Rodembusch, *Photochemical & Photobiological Sciences*, 2018, **17**, 231-238.
5. A. Onufriev, D. A. Case and G. M. Ullmann, *Biochemistry*, 2001, **40**, 3413-3419.
6. C. Lawler and M. D. Fayer, *The Journal of Physical Chemistry B*, 2015, **119**, 6024-6034.
7. E. Pines and D. Huppert, *The Journal of Chemical Physics*, 1986, **84**, 3576-3577.
8. N. Agmon, D. Huppert, A. Masad and E. Pines, *J. Phys. Chem.*, 1991, **95**, 10407-10413.
9. C. Spies, S. Shomer, B. Finkler, D. Pines, E. Pines, G. Jung and D. Huppert, *Phys. Chem. Chem. Phys.*, 2014, **16**, 9104-9114.
10. T. Jang, G. Lee, S. Lee, J. Lee and Y. Pang, *J. Mol. Liq.*, 2019, **279**, 503-509.
11. A. Shabbir, T. Jang, G. Lee and Y. Pang, *J. Mol. Liq.*, 2022, **346**, 118313.
12. A. Phukon and K. Sahu, *Chem. Commun.*, 2015, **51**, 14103-14106.
13. A. Phukon, N. Barman and K. Sahu, *Langmuir*, 2015, **31**, 12587-12596.
14. D. B. Spry, A. Goun and M. D. Fayer, *J. Phys. Chem. A*, 2007, **111**, 230-237.
15. D. B. Spry, A. Goun, K. Glusac, D. E. Moilanen and M. D. Fayer, *J. Am. Chem. Soc.*, 2007, **129**, 8122-8130.
16. W. Heo, N. Uddin, J. W. Park, Y. M. Rhee, C. H. Choi and T. Joo, *Phys. Chem. Chem. Phys.*, 2017, **19**, 18243-18251.
17. T. Mondal, A. K. Das, D. K. Sasmal and K. Bhattacharyya, *J. Phys. Chem. B*, 2010, **114**, 13136-13142.
18. L. Giestas, C. Yihwa, J. C. Lima, C. Vautier-Giongo, A. Lopes, A. L. Maçanita and F. H. Quina, *J. Phys. Chem. A*, 2003, **107**, 3263-3269.
19. T. H. Tran-Thi, T. Gustavsson, C. Prayer, S. Pommeret and J. T. Hynes, *Chem. Phys. Lett.*, 2000, **329**, 421-430.
20. O. F. Mohammed, J. Dreyer, B.-Z. Magnes, E. Pines and E. T. J. Nibbering, *ChemPhysChem*, 2005, **6**, 625-636.